Progress In Electromagnetics Research C, Vol. 107, 259–271, 2021

On Application of Taper Windows for Sidelobe Suppression in LFM Pulse Compression

Volodymyr G. Galushko*

Abstract—The efficiency of the standard tapered windows as applied to sidelobe suppression in compressed pulses with linear frequency modulation (LFM) or chirp pulses corresponds to the literature data only in the case of rather great values of the pulse duration-bandwidth product $B \geq 100$. With comparatively small values of B (several dozens or so), the side-lobe levels prove to be essentially greater than those announced in the literature. In the paper, the output signal of the chirp-pulse compression filter is analyzed in order to look into causes of the discrepancy between the sidelobe level obtainable using standard tapered windows and the literature data. Expressions are derived for estimating the maximum number of zeros and maxima in the response of the optimum filter of chirp-pulse compression and separation between adjacent and "like" (with the same numbers) zeros and maxima in dependence on the signal duration-bandwidth product. The amount of loss in the signal-to-noise ratio due to the application of smoothing functions is determined. The case of applying window functions in the form of cosine harmonics of the Fourier series, which describes a rather great number of the standard windows, is analyzed in detail. Analytical expressions are presented for the output signal of the chirp-pulse compression filter on the basis of such windows and the amount of loss in the signal-to-noise ratio. A comparative analysis of the Hamming and Blackman windows is made in dependence on B. It is shown that application of the Hamming window is more efficient up to $B \approx 80$. For greater values of B, the Blackman window shows a higher efficiency. As B increases, the efficiency of both windows steadily increases asymptotically approaching the figure declared in the literature. Coefficients of window functions containing 2 cosine harmonics of the Fourier series have empirically been selected which made it possible to reduce the sidelobe level by approximately 0.34 dB for $B = 21$ and by more than 1 dB for $B = 7$ as compared with the Hamming window. The obtained results allow concluding that the optimization problem for the window function parameters in the case of small values of the pulse duration-bandwidth product should be solved individually for each specific value of B. Most likely it would be impossible to obtain the extremely low sidelobe level; however, a certain improvement of the characteristics of the chirp-pulse compression filter seems quite possible.

1. INTRODUCTION

As known [1], selection of the signal parameters for pulse radars represents a certain compromise between providing the range resolution as high as possible, on the one hand, and maximum detection range, on the other hand. The first requirement can be satisfied through the use of rather short pulses, while the maximum detection range is determined by the radar performance figure and can be enhanced through either lengthening the sounding signal or increasing the radar peak power. Since the peak power is limited by purely technical feasibility, the only way to satisfy these contradicting requirements is the use of complex signals with great duration-bandwidth products $B = \Delta f \tau_p \gg 1$, where Δf and τ_p are the signal bandwidth and duration, respectively [2]. In this case, a radar transmits a rather long

Received 19 August 2020, Accepted 10 December 2020, Scheduled 24 December 2020
* Corresponding author: Volodymyr G. Galushko (galushko@rian.kharkov.ua).
The author is with the Institute of Radio Astronomy, National Academy of Sciences of Ukraine, 4, Mystetstv St., Kharkiv 61002, Ukraine.

pulse whose phase or frequency changes with time following a certain law to obtain the signal spectrum width Δf which would provide a specified spatial resolution [3]. The target echo is processed with the optimal filter whose output represents a nonmodulated signal with the magnitude proportional to the transmitted pulse power and duration equal to about $1/\Delta f$.

Among a great variety of complex radar signals [1, 4], the most widely used are pulses with linear frequency modulation (LFM). This is explained by a comparative simplicity of implementation of algorithms for generating and optimal processing of such signals which suggest a number of other beneficial properties [1], for example, tolerance to Doppler frequency shifts [3]. The most essential shortcoming of LFM-pulses in radar applications is a rather high side-lobe level in the pulse compression filter output. For example, the first sidelobe is only about -13 dB with respect to the main maximum [1]. This effect can mask echoes from weak targets against strong reflections from other targets or clutter. For this reason, one of the basic problems is sidelobe suppression which is commonly solved through the use of various taper windows in the time or frequency domain [1]. The charge for sidelobe reduction is broadening of the main maximum and decrease in the signal-to-noise ratio (SNR). It should be noted that the vast majority of the applied window functions, whose rather complete nomenclature can be found, e.g. in [5], have been developed for estimating spectral amplitudes of narrowband signals. Their efficiency as applied to sidelobe suppression in compressed LFM pulses is open to certain questions, especially in the case of comparatively small B. Thus, results presented in [6, 7] show that with $B < 50$ the sidelobe level provided by the Hamming window is essentially higher than -42.8 dB announced in the literature (see, e.g. [1, 5]).

Some authors [1, 8] suppose that such a discrepancy between the declared and real sidelobe levels is due to an essential difference of the LFM pulse spectrum shape from a rectangular one, which increases with decreasing B and suggests various algorithms of its correction. However, it has not succeeded to essentially improve the compression filter characteristics in this way. Probably, the reason is that such an approach is very similar to the spectral domain smoothing which, judging from results presented in [7], is less efficient than the time domain one. Moreover, artificial limitation of the spectrum results in that the response of the compression filter occupies the whole range of possible time-delays since the Fourier transform of a finite spectrum represents a function of infinite duration. This can result in an essential decrease of the signal-to-clutter ratio.

Thus, the reason for insufficient efficiency of applying standard taper windows for reducing the sidelobe level of the LFM pulse compression filter is hidden in the structure of the signal itself rather than in the discrepancy of its spectrum shape from a rectangular one. The present paper is aimed at testing this assumption and developing recommendations on selecting time-domain taper functions for the suppression of LFM pulse sidelobes in the case of small duration-bandwidth products.

The rest of the paper is organized as follows. In Section 2, formulas are derived for the output of the LFM pulse compression filter with an arbitrary time-domain tapered window, and it is shown that the output represents a Fourier transform of the taper function with variable integration limits. Section 3 presents an analysis of the amount of loss in the signal-to-noise ratio due to applying taper windows. In Section 4, the structure of the optimal pulse compression filter output is considered in order to find the reasons for the discrepancy between the announced in the literature and actual degree of sidelobe suppression in the optimal LFM pulse compression filter using standard taper windows. Section 5 presents analytical expressions derived for the output signal and amount of loss in the signal-to-noise ratio of the chirp-pulse compression filter on the basis of the taper window function in the form of cosine harmonics of the Fourier series, which describes a rather great number of the standard windows. In Section 6, a comparative analysis of the Hamming and Blackman windows is done in dependence on the pulse duration-bandwidth product B, and two windows with empirically selected parameters are suggested which have advantage over the two first for $B = 21$ and $B = 7$. Finally, concluding remarks and possible future research tracks are outlined in Section 7.

2. OUTPUT OF THE LFM PULSE COMPRESSION FILTER WITH A TIME-DOMAIN TAPER WINDOW

Let a radar transmission be a rectangular LFM pulse as follows

$$S_0(t) = A_0(t)e^{-i[\omega_0(t-\tau_p/2)+\mu(t-\tau_p/2)^2/2+\varphi_0]}. \tag{1}$$

Here $A_0(t) = \begin{cases} A_0, & t \in [0, \tau_p]; \\ 0, & t \notin [0, \tau_p]; \end{cases}$ with A_0 and τ_p being the pulse amplitude and duration, respectively; $\omega_0 = 2\pi f_0$ is the carrier frequency; $\mu = 2\pi\Delta f/\tau_p$ is the slope of the phase modulation, with Δf being the frequency sweep width; and φ_0 is the initial phase.

The signal $S_T(t)$ reflected from a fixed point target will differ from Eq. (1) by its amplitude $A_T(t)$, phase φ_T and will be time-delayed by the value $\tau_d = 2R_T/c$, with R_T being the target range and c the light speed, *viz.*

$$S_T(t) = A_T(t)e^{-i[\omega_0(t-\tau_d-\tau_p/2)+\mu(t-\tau_d-\tau_p/2)^2/2+\varphi_T]}. \tag{2}$$

Here $A_T(t) = \begin{cases} \gamma A_0, & t \in [\tau_d, \tau_d + \tau_p]; \\ 0, & t \notin [\tau_d, \tau_d + \tau_p]; \end{cases}$ where γ is a factor to characterize the target reflectivity and power loss on the signal traveling from the radar to the target and back.

As known [1, 3], the optimal compression algorithm for signal Eq. (2) consists in its convolution with the reference signal given by (1). In practice, the convolution integral is more convenient to be calculated in the spectral domain based on the convolution theorem [9], having previously multiplied the reference signal by a weight function $w(t)$ to reduce the compression filter sidelobes. Thus, the output $S_{Tw}(t)$ of the pulse compression filter with a time-domain taper window can be represented as

$$S_{Tw}(t) = \int\limits_{-\infty}^{\infty} S_{rw}^*(\omega)S_T(\omega)e^{-i\omega t}\mathrm{d}\omega. \tag{3}$$

Here

$$S_{rw}(\omega) = \frac{1}{2\pi}\int\limits_0^{\tau_p} w(t)e^{i[\omega t-\omega_0(t-\tau_p/2)-\mu(t-\tau_p/2)^2/2]}\mathrm{d}t \tag{4}$$

is the Fourier transform of the product of the reference signal Eq. (1) with $A_0 = 1$ to obtain the correct dimension and a taper window $w(t)$, and the asterisk "$*$" stands for complex conjugation;

$$S_T(\omega) = \frac{\gamma A_0}{2\pi}\int\limits_0^{\tau_p} e^{i[\omega(t+\tau_d)-\omega_0(t-\tau_p/2)-\mu(t-\tau_p/2)^2/2]}\mathrm{d}t \tag{5}$$

is the Fourier transform of the target echo Eq. (2).

Substitution of Eqs. (4) and (5) into Eq. (3) yields

$$S_{Tw}(t) = \frac{\gamma A_0}{2\pi}\int\limits_0^{\tau_p}\int\limits_0^{\tau_p} w(t')e^{i[\omega_0(t'-t'')+\mu(t'^2-t''^2-t'\tau_p+t''\tau_p)/2]}\delta(t''-t'+\tau_d-t)\mathrm{d}t'\mathrm{d}t'', \tag{6}$$

where $\delta(x) = \frac{1}{2\pi}\int\limits_{-\infty}^{\infty} e^{i\omega x}\mathrm{d}\omega$ is the Dirac delta function.

Changing the integration variables to the sum $\xi = t'' + t' - \tau_p$ and difference $\rho = t'' - t'$ ones and introducing the time $\tilde{t} = t - \tau_d$, we can write Eq. (6) as

$$S_{Tw}(\tilde{t}) = \frac{\gamma A_0}{4\pi}\left\{\int\limits_{-\tau_p}^{0}\int\limits_{-\rho-\tau_p}^{\rho+\tau_p} + \int\limits_{0}^{\tau_p}\int\limits_{\rho-\tau_p}^{-\rho+\tau_p}\right\} w[(\xi-\rho+\tau_p)/2]e^{-i(\omega_0\rho+\mu\rho\xi/2)}\delta(\rho-\tilde{t})\mathrm{d}\rho\mathrm{d}\xi. \tag{7}$$

As can be seen, the first term in Eq. (7) contributes to the pulse compression filter output $S_{Tw}(\tilde{t})$ for $-\tau_p \le \tilde{t} \le 0$, while the second for $\tau_p \ge \tilde{t} \ge 0$. Then, making use of the sifting property of the Dirac delta function and changing the variables $\xi - \rho + \tau_p = 2\zeta$, we finally obtain

$$\underset{-\tau_p\le\tilde{t}\le 0}{S_{Tw}(\tilde{t})} = \frac{\gamma A_0}{2\pi}e^{-i[\omega_0\tilde{t}+\mu\tilde{t}(\tilde{t}-\tau_p)/2]}\int\limits_{-\tilde{t}}^{\tau_p} w(\varsigma)e^{-i\mu\tilde{t}\varsigma}\mathrm{d}\varsigma, \tag{8a}$$

$$\underset{\tau_p\geq\tilde{t}\geq 0}{S_{Tw}(\tilde{t})} = \frac{\gamma A_0}{2\pi} e^{-i[\omega_0\tilde{t}+\mu\tilde{t}(\tilde{t}-\tau_p)/2]} \int\limits_0^{\tau_p-\tilde{t}} w(\varsigma) e^{-i\mu\tilde{t}\varsigma} \mathrm{d}\varsigma. \tag{8b}$$

It can easily be shown that with $w(\varsigma) = 1$ (no taper window) Equation (8) is reduced up to a constant factor to the well-known formula for the correlation function of LFM pulses [4]

$$\underset{|\tilde{t}|\leq\tau_p}{S_{T0}(\tilde{t})} = \frac{\gamma A_0}{2\pi}(\tau_p - |\tilde{t}|)\mathrm{sinc}[\mu\tilde{t}(\tau_p - |\tilde{t}|)/2]e^{-i\omega_0\tilde{t}}, \tag{9}$$

where $\mathrm{sinc}(x) = \sin(x)/x$.

As follows from Eq. (8), the response $S_{Tw}(\tilde{t})$ of the LFM pulse compression filter with a time-domain tapering can be regarded as a Fourier transform of the taper function $w(\varsigma)$ with variable integration limits. On the other hand, in the case of applying standard windows for estimating spectral amplitudes [5] integration is performed within fixed limits $[0, T]$, where T is the observation interval. It is quite possible that this is the reason for insufficient efficiency of applying standard window functions for sidelobe reduction in the case of LFM pulses. To verify this assumption, it is necessary to thoroughly investigate the structure of the pulse compression filter output which will be done in Section 4. But first let us estimate the amount of loss in the signal-to-noise ratio associated with applying taper windows.

3. AMOUNT OF LOSS IN THE SIGNAL-TO-NOISE RATIO DUE TO APPLYING TAPER WINDOWS

As follows from Eq. (9), the output signal of the optimal compression filter of LFM pulses is maximum with $\tilde{t} = 0$, which corresponds to the propagation time τ_d of the sounding pulse to the target and back. Quite evidently, $S_{Tw}(\tilde{t})$ should be maximum with $\tilde{t} = 0$ in order that the estimate of the target range $R_T = c\tau_d/2$ is unbiased. For this reason, in the capacity of the signal-to-noise ratio we will consider the quotient

$$SNR_w = \frac{|S_{Tw}(0)|^2}{\sigma_{Tw}^2}, \tag{10}$$

where σ_{Tw}^2 is the contribution of the radar receiver noise to the output signal.

According to Eq. (8) the nominator of Eq. (10) is

$$|S_{Tw}(0)|^2 = \left(\frac{\gamma A_0}{2\pi}\right)^2 \int\limits_0^{\tau_p}\int\limits_0^{\tau_p} w(\varsigma)w^*(\varsigma')\mathrm{d}\varsigma\mathrm{d}\varsigma' = \left(\frac{\gamma A_0}{2\pi}\left|\int\limits_0^{\tau_p} w(\varsigma)\mathrm{d}\varsigma\right|\right)^2. \tag{11}$$

To calculate σ_{Tw}^2, let us make use of the model of a stationary noise $n(t)$ with zero mean, $\langle n(t)\rangle = 0$ (angular brackets mean statistical averaging), and correlation function, $K(t_2 - t_1) = \langle n(t_1)n^*(t_2)\rangle$.

Since the output signal represents a convolution of the reference and received signals, we can immediately write

$$\sigma_{Tw}^2 = \frac{1}{4\pi^2} \int\limits_{-\tau_p/2}^{\tau_p/2}\int\limits_{-\tau_p/2}^{\tau_p/2} w(t_1 + \tau_p/2)w^*(t_2 + \tau_p/2)K(t_2 - t_1)e^{-i[\omega_0(t_2-t_1)+\mu(t_2^2-t_1^2)/2]}\mathrm{d}t_1\mathrm{d}t_2.$$

Changing the integration variables to the sum $\xi = t_2 + t_1$ and difference $\rho = t_2 - t_1$ and assuming $K(\rho)$ to be a rather sharp function with the characteristic scale (correlation length) l much less than the pulse length τ_p,

$$l/\tau_p \ll 1, \tag{12}$$

we obtain

$$\sigma_{Tw}^2 \approx \frac{1}{8\pi^2} \int\limits_{-\tau_p}^{\tau_p}\int\limits_{-\infty}^{\infty} w[(\xi - \rho + \tau_p)/2]w^*[(\xi + \rho + \tau_p)/2]K(\rho)e^{-i[\omega_0+\mu\xi/2]\rho}\mathrm{d}\xi\mathrm{d}\rho. \tag{13}$$

If the window function $w(t)$ is sufficiently smooth with the characteristic variation scale much greater than l, we can consider within the linear approximation that

$$w[(\xi \pm \rho + \tau_p)/2] \approx w[(\xi + \tau_p)/2] \pm \rho \left. \frac{\mathrm{d}w[(\xi \pm \rho + \tau_p)/2]}{\mathrm{d}\rho} \right|_{\rho=0}$$

and represent Eq. (13) to the second-order terms as

$$\sigma_{Tw}^2 \approx \frac{1}{8\pi^2} \int\limits_{-\tau_p}^{\tau_p} |w[(\xi + \tau_p)/2]|^2 \mathrm{d}\xi \int\limits_{-\infty}^{\infty} K(\rho) e^{-i[\omega_0 + \mu\xi/2]\rho} \mathrm{d}\rho. \tag{14}$$

The inner integral over ρ in Eq. (14) represents the noise power spectrum. In the case of a uniform distribution within the receiver bandpass, it is characterized by the spectral power density $N_0/2$. Thus, finally we have

$$\sigma_{Tw}^2 \approx \frac{N_0}{4\pi} \int\limits_{0}^{\tau_p} |w(\xi)|^2 \mathrm{d}\xi. \tag{15}$$

Substitution of Eqs. (11) and (15) into Eq. (10) yields

$$SNR_w \approx \frac{\gamma^2 A_0^2}{\pi N_0} \frac{\left| \int\limits_{0}^{\tau_p} w(\xi) \mathrm{d}\xi \right|^2}{\int\limits_{0}^{\tau_p} |w(\xi)|^2 \mathrm{d}\xi}. \tag{16}$$

The signal-to-noise ratio SNR_0 in the case of no tapering, i.e., with $w(\xi) = 1$ in Eq. (16), is

$$SNR_0 \approx \frac{\gamma^2 A_0^2 \tau_p}{\pi N_0}. \tag{17}$$

Hence, dividing Eq. (16) by Eq. (17) we obtain an estimate of the amount of loss in the signal-to-noise ratio, $\Gamma = SNR_w/SNR_0$, due to applying a taper window, *viz.*

$$\Gamma = \frac{1}{\tau_p} \frac{\left| \int\limits_{0}^{\tau_p} w(\xi) \mathrm{d}\xi \right|^2}{\int\limits_{0}^{\tau_p} |w(\xi)|^2 \mathrm{d}\xi}. \tag{18}$$

In conclusion of this Section, let us analyze the conditions under which inequality Eq. (12) holds. In the case of a uniformly distributed noise at the receiver input ("white" noise model), its correlation length l is determined by the receiver bandpass $\Delta f_{rec} (l \approx 1/\Delta f_{rec})$. To provide optimal filtering, the latter should be approximately equal to the LFM pulse frequency sweep Δf. Thus, inequality Eq. (12) is identical to the condition

$$\tau_p / l \approx \tau_p \Delta f \gg 1.$$

In other words, it is met in the case of signals with great duration-bandwidth products $B = \tau_p \Delta f \gg 1$. Accordingly, the estimate given by Eq. (18) is correct for $B \gg 1$.

4. ANALYSIS OF THE STRUCTURE OF THE OPTIMAL PULSE COMPRESSION FILTER OUTPUT

To find the reasons for the discrepancy between that presented in the literature and actual degree of sidelobe suppression in the optimal LFM pulse compression filter using standard taper windows, let us analyze the structure of this filter output $S_{T0}(t)$. (Here and below we drop the symbol tilde over t.) As follows from Eq. (8) with $w(\xi) = 1$, the filter output $S_{T0}(t)$ can be regarded as a Fourier transform of a rectangular window with variable length. As a result, minima (zeros) and maxima of the $S_{T0}(t)$ envelope are located non-uniformly in contrast to the ordinary Fourier spectrum with a fixed window width. Indeed, positions of minima in $|S_{T0}(t)|$ are determined from the equation

$$\mu t(\tau_p - |t|) = 2\pi n, \quad |t| \le \tau_p, \tag{19}$$

where $n = \pm 1, \pm 2, \ldots, n_{\max}$ numbers minima in the $|S_{T0}(t)|$ function, with the positive n correspondent to $0 \le t \le \tau_p$, while the negative to $-\tau_p \le t \le 0$. Because of symmetry of $|S_{T0}(t)|$ about $t = 0$, it is sufficient to consider one branch of numbers n, for example, positive. In this case, the solution of Equation (19) is

$$t_{1,2}^{\min} = \frac{\tau_p}{2}\left[1 \pm \sqrt{1 - \frac{4n}{B}}\right]. \tag{20}$$

As can be seen from Eq. (20), there are two minima for each n located symmetrically about $t = \tau_p/2$. The maximum number of minima is limited by the inequality

$$n_{\max} \le B/4.$$

If $B/4$ is equal to an integer number M, then minima corresponding to $n = M$ merge at the point $t = \tau_p/2$ and hence $|S_{T0}(\tau_p/2)| = 0$ (see Fig. 1(a)). With $B/4 = M + 1$ a local maximum is observed at this point (see Fig. 1(b)), which slightly broadens when $B/4 = M + 2$ (see Fig. 1(c)) and then, with $B/4 = M + 3$, is transformed into a local minimum (see Fig. 1(d)).

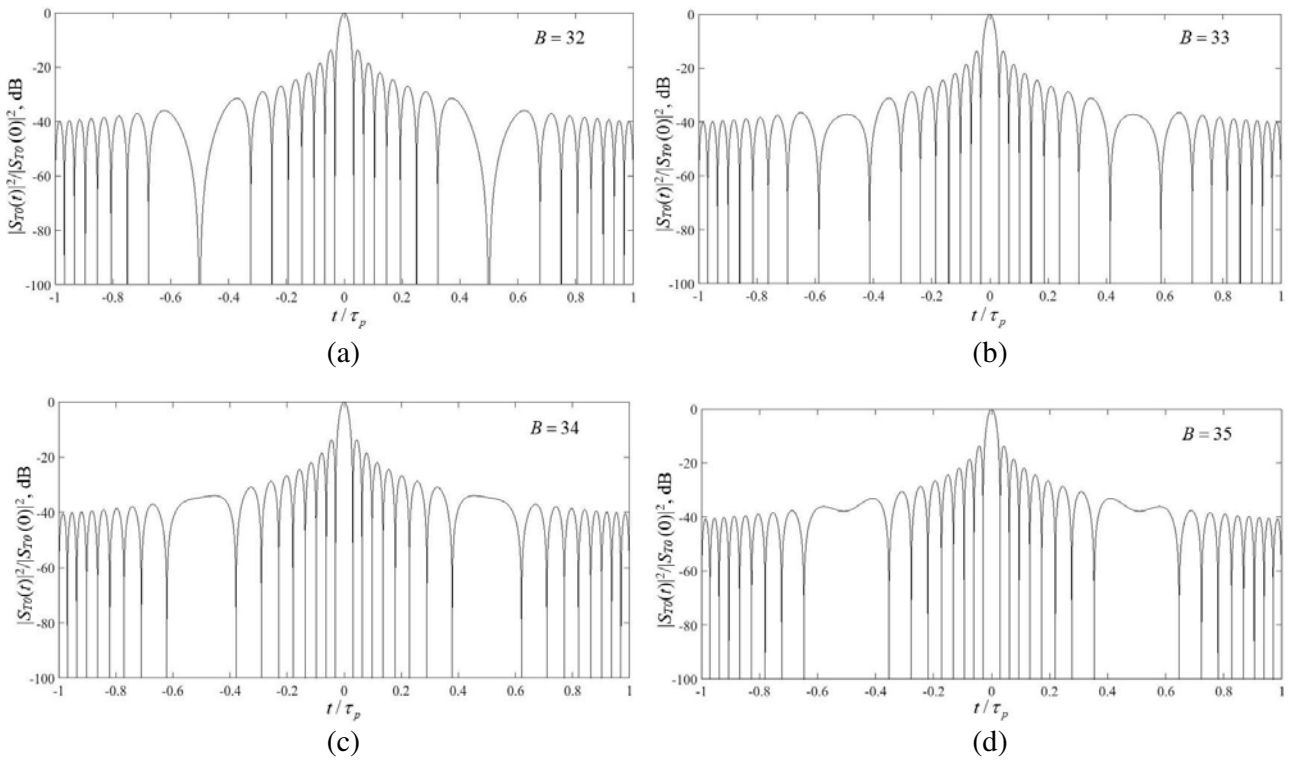

Figure 1. Output signal of the optimal LFM pulse compression filter for $\Delta f = 10\,\text{MHz}$ and (a) $\tau_p = 3.2\,\mu\text{s}$ ($B = 32$), (b) $\tau_p = 3.3\,\mu\text{s}$ ($B = 33$), (c) $\tau_p = 3.4\,\mu\text{s}$ ($B = 34$) and (d) $\tau_p = 3.5\,\mu\text{s}$ ($B = 35$).

The zero-level width of the main maximum of the function $|S_{T0}(t)|$ is equal to

$$\Delta t = \tau_p \left[1 - \sqrt{1 - \frac{4}{B}}\right].$$

The separation between adjacent minima, $\Delta t^{\min}_{n+1,n} = t^{\min}(n+1) - t^{\min}(n)$, for $4n/B \ll 1$ can be estimated up to quadratic terms after the formula

$$|\Delta t^{\min}_{n+1,n}| \approx \frac{1}{\Delta f}\left(1 + \frac{2n+1}{B}\right).$$

Positions of maxima in $|S_{T0}(t)|$ can be estimated in a similar way. Thus, considering the interval $0 \le t \le \tau_p$ we obtain that maxima of $|S_{T0}(t)|$, similar to minima, are located symmetrically about $t = \tau_p/2$ at the points

$$t^{\max}_{1,2} = \frac{\tau_p}{2}\left[1 \pm \sqrt{1 - \frac{2(2m+1)}{B}}\right],$$

where m is the maximum number, whence it follows that the maximum number of peaks $m_{\max}$ satisfies the inequality

$$m_{\max} \le \frac{1}{2}\left(\frac{B}{2} - 1\right).$$

With $4m/B \ll 1$, the separation between adjacent maxima, $\Delta t^{\max}_{m+1,m} = t^{\max}(m+1) - t^{\max}(m)$, is equal up to quadratic terms to

$$|\Delta t^{\max}_{m+1,m}| \approx \frac{1}{\Delta f}\left(1 + \frac{2(m+1)}{B}\right).$$

Most likely, the dependence of the separation between adjacent minima and maxima of the $|S_{T0}(t)|$ function on time t is the reason for the essential difference of the actual sidelobe level in the case of applying standard taper windows from that declared in the literature. Indeed, standard taper windows work well if the separation between adjacent minima and maxima of the analyzed function is fixed ($\Delta t^{\min}_{n+1,n} = \text{const}$, $\Delta t^{\max}_{m+1,m} = \text{const}$), which is the case of spectral analysis of narrowband signals for which these, in fact, have been developed. Since values of $\Delta t^{\min}_{n+1,n}$ and $\Delta t^{\max}_{m+1,m}$ are inversely proportional to the LFM pulse duration-bandwidth product B, with $B \gg 1$ these change quite slowly. As a result, standard windows to a sufficient extent suppress the sidelobes lying within the interval from $t^{\max}(m=1)$ to the time moment t_{cut} when $\Delta t^{\min}_{n+1,n}$ and $\Delta t^{\max}_{m+1,m}$ increase to such a degree that the applied window becomes less effective. However, the sidelobes decrease by that moment to such an extent that there is no need to suppress them. Accordingly, the degree of sidelobe suppression approaches that declared in the literature as B increases. With comparatively small values of B, the separation $\Delta t^{\max}_{m+1,m}$ changes quite rapidly, and standard windows lose their efficiency for small m when the sidelobe level remains rather high. As an example, Fig. 2 presents dependences $|S_{T0}(t)|$ (upper panels) and $|S_{Tw}(t)|$ (lower panels) calculated for $B = 32$ (left panels) and $B = 320$ (right panels). The pulse length τ_p in both cases is equal to 3.2 µs. The Hamming window [5] $w(t) = \alpha - (1-\alpha)\cos(2\pi t/\tau_p)$ with $\alpha = 0.53836$ is used as the taper one. As can be seen for $B = 320$, the Hamming window practically provides the degree of sidelobe suppression presented in the literature (the first sidelobe is about -42.49 dB). Nevertheless, its efficiency noticeably decreases within a rather wide range near $t = \pm\tau_p/2$ such that one can see even somewhat increase in the sidelobe level in contrast to monotonous decrease in the case of calculation of the Fourier spectrum of a monochromatic signal (see Fig. 3). For example, at $t/\tau_p \approx \pm 0.46$ (approximately 80-th maximum of $|S_{T0}(t)|$), the output signal of the pulse compression filter with the Hamming window is equal to -53.42 dB, while without tapering it makes -53.31 dB. However, it is already unimportant since the sidelobe level within this interval is much lower than ≈ -42.7 dB declared in the literature [1, 5]. At the same time with $B = 32$, the separation $\Delta t^{\max}_{m+1,m}$ noticeably increases already starting from $m = 6$, and the Hamming window loses its efficiency in the range where the sidelobes of the optimal pulse compression filter without tapering are still rather high (the 6-th sidelobe is about -26.9 dB). As a result, the maximum value of $|S_{Tw}(t)|$ outside the main maximum is as high as nearly -32.7 dB.

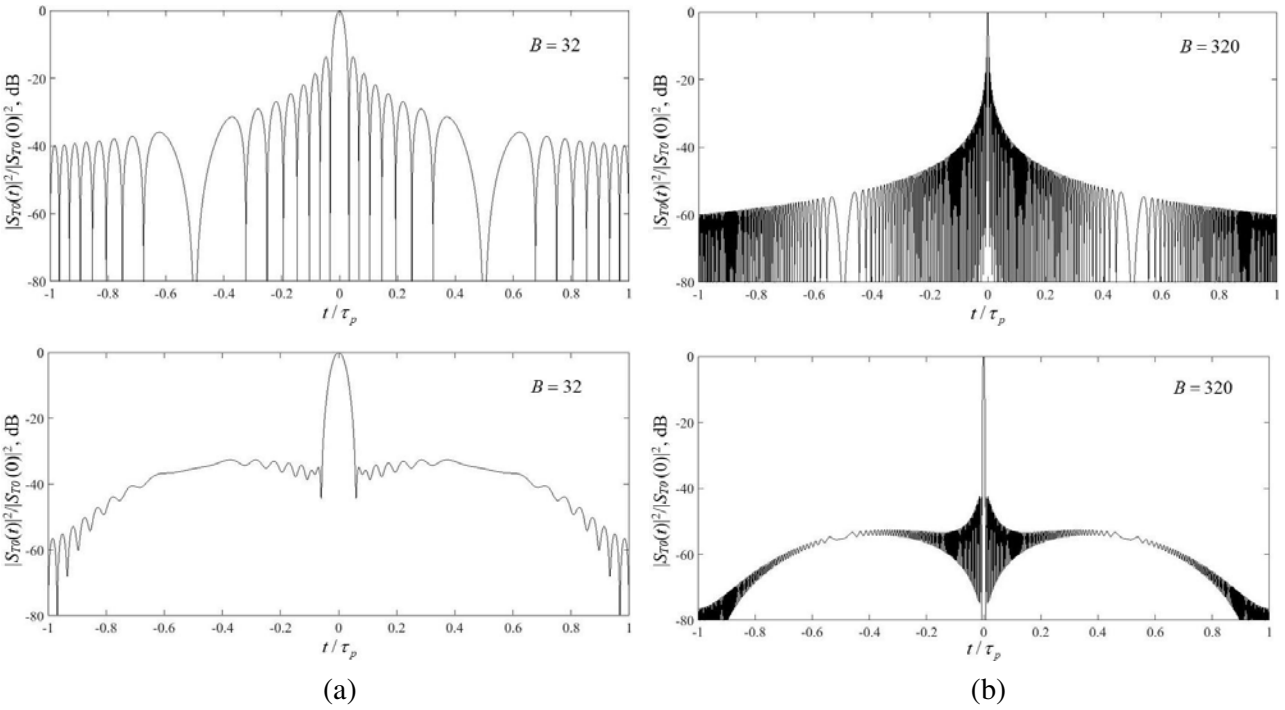

Figure 2. Output of the LFM pulse compression filter without tapering (upper panels) and with Hamming taper window (lower panels) calculated for the pulse length (a) $\tau_p = 3.2\,\mu$s and (b) $B = 32$ and $B = 320$.

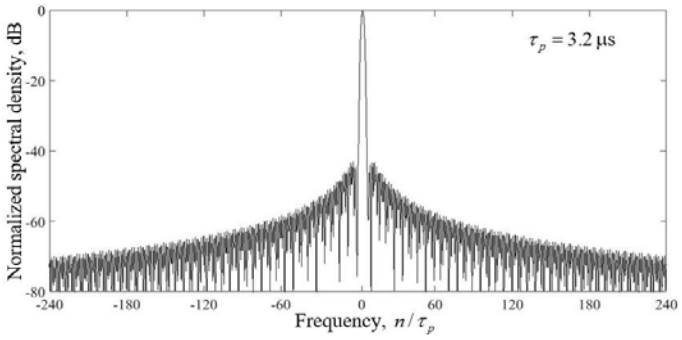

Figure 3. Normalized spectrum of a harmonic signal calculated over the pulse length $\tau_p = 3.2\,\mu$s with Hamming window tapering. Zero on the frequency axis corresponds to the carrier frequency.

Since the Hamming window parameters, equally as those of other standard windows, have been selected for the case of equidistant sidelobes, it is quite possible that the situation can be somewhat improved through selecting their values purposefully for sidelobe suppression in the LFM pulse compression filter. In the next section, we will investigate this issue by way of example of window functions as follows $w(t) = \sum_{k=0}^{K} a_k \cos(2\pi kt/\tau_p)$ which are most frequently used in radar signal processing and will try to develop some recommendations on selecting their parameters.

5. CHARACTERISTICS OF THE TAPER WINDOWS IN THE FORM $w(t)=\sum_{k=0}^{K} a_k \cos(2\pi k t/\tau_p)$

After the change of variable in Eq. (8), $\xi = y + \tau_p/2$, we obtain the following formula for the absolute value of the output signal of the pulse compression filter with a taper window $w(t)$

$$\underset{|t|\le\tau_p}{|S_{Tw}(t)|} = \frac{\gamma A_0}{2\pi}\left|\int\limits_{-\tau_p/2}^{\tau_p/2-|t|} w(\tau_p/2 \pm y)e^{-i\mu|t|y}\mathrm{d}y\right|, \tag{21}$$

where the signs "+" and "−" correspond to positive and negative values of t, respectively.

As follows from Eq. (21), in order that the function $|S_{Tw}(t)|$ be symmetric about $t = 0$, the taper function $w(t)$ should be symmetric about the pulse middle $\tau_p/2$. Supposing that the symmetry condition is met, in what follows we will consider the time range $\tau_p \ge t \ge 0$ only. Let us introduce a dimensionless time $t' = t/\tau_p$ and proceed in Eq. (8b) to the dimensionless variable of integration $\eta = \varsigma/\tau_p$. Then we can write

$$\underset{0\le t'\le 1}{|S_{Tw}(t')|^2} = \left(\frac{\gamma A_0\tau_p}{2\pi}\right)^2 \int\limits_0^{1-t'}\int\limits_0^{1-t'} w(\eta_1)w^*(\eta_2)e^{-i2\pi Bt'(\eta_1-\eta_2)}\mathrm{d}\eta_1\mathrm{d}\eta_2.$$

All the known taper functions $w(t)$ are real [7, 8], and thus we have

$$\underset{0\le t'\le 1}{|S_{Tw}(t')|^2} = \left(\frac{\gamma A_0\tau_p}{2\pi}\right)^2 \left\{\left[\int\limits_0^{1-t'} w(\eta)\cos(2\pi Bt'\eta)\mathrm{d}\eta\right]^2 + \left[\int\limits_0^{1-t'} w(\eta)\sin(2\pi Bt'\eta)\mathrm{d}\eta\right]^2\right\}. \tag{22}$$

Let us represent $w(\eta)$ as a Fourier series of K harmonics

$$w(\eta) = a_0 + \sum_{k=1}^{K}[a_k\cos(2\pi k\eta) + b_k\sin(2\pi k\eta)],$$

where η varies between 0 and 1.

The condition of window symmetry about the pulse center is identical to fulfillment of the equality

$$w(0.5 + \Delta\eta) = w(0.5 - \Delta\eta),$$

whence it follows that $b_k = 0$. Consequently we obtain

$$w(\eta) = \sum_{k=0}^{K} a_k\cos(2\pi k\eta). \tag{23}$$

Note that Eq. (23) describes a wide class of taper functions which are frequently used in various applications, including radars. In dependence on the number of series terms K and values of the coefficients a_k, this class is represented by the Hanning, Hamming, and Blackman windows, Flat-Top-Window, etc. [5].

After rather simple but cumbersome calculations, substitution of Eq. (23) into Eq. (22) yields

$$\begin{aligned}
\underset{0\le t'\le 1}{|S_{Tw}(t')|^2} \;=\; & \left(\frac{\gamma A_0\tau_p}{4\pi^2}\right)^2 \left\{\left(\frac{2a_0}{Bt'}\right)^2 \sin^2[\pi Bt'(1-t')] + \frac{4a_0\sin[\pi Bt'(1-t')]}{Bt'}\right. \\
& \times \sum_{k=1}^{K} a_k\left[\frac{\sin[\pi(k-Bt')(1-t')]}{k-Bt'} + \frac{\sin[\pi(k+Bt')(1-t')]}{k+Bt'}\right]\cos[\pi k(1-t')] \\
& + \frac{1}{2}\sum_{k,l=1}^{K} a_k a_l\left\{\cos[\pi(1-t')(k-l)]\left[\frac{\sin[\pi(k-Bt')(1-t')]\sin[\pi(l-Bt')(1-t')]}{(k-Bt')(l-Bt')}\right.\right. \\
& \left.\left. + \frac{\sin[\pi(k+Bt')(1-t')]\sin[\pi(l+Bt')(1-t')]}{(k+Bt')(l+Bt')}\right] + \cos[\pi(1-t')(k+l)]\right.
\end{aligned}$$

$$\times \left[\frac{\sin[\pi(k+Bt')(1-t')]\sin[\pi(l-Bt')(1-t')]}{(k+Bt')(l-Bt')} + \frac{\sin[\pi(k-Bt')(1-t')]\sin[\pi(l+Bt')(1-t')]}{(k-Bt')(l+Bt')} \right] \Bigg\} \Bigg\}. \quad (24)$$

The noise contribution to the output of the pulse compression filter with the taper window in Eq. (23) can be estimated after Eq. (15). The result of rather simple calculations is

$$\sigma_{Tw}^2 \approx \frac{N_0\tau_p}{4\pi}\left(a_0^2 + \frac{1}{2}\sum_{k=1}^{K} a_k^2\right). \quad (25)$$

Having divided Eq. (24) with $t' = 0$ by Eq. (25), we obtain the following formula for the signal-to-noise ratio at the output of the LFM pulse compression filter with the taper window given by Eq. (23)

$$SNR_w \approx \frac{\gamma^2 A_0^2 \tau_p}{\pi N_0} \frac{a_0^2}{a_0^2 + \frac{1}{2}\sum_{k=1}^{K} a_k^2}. \quad (26)$$

Now, let us estimate the amount of loss in the signal-to-noise ratio associated with the use of taper window given by Eq. (23). Division of Eq. (26) by Eq. (17) yields

$$\Gamma \approx \frac{a_0^2}{a_0^2 + \frac{1}{2}\sum_{k=1}^{K} a_k^2}. \quad (27)$$

As follows from Eq. (27), a dilemma is faced when selecting a taper window between the complexity of the window shape (number of terms in series Eq. (23)), which to a certain extent determines the degree of sidelobe suppression, and the amount of loss in the signal-to-noise ratio. Also, it should be taken into account that the efficiency of applying standard taper windows decreases essentially in the case of small duration-bandwidth products B. Hence, it may prove necessary to solve the problem of selecting the taper window parameters individually for each specific value of B. To illustrate the issue stated above, let us perform a comparative analysis of the output signals of the LFM pulse compression filters with the Hamming and Blackman windows, and also develop some recommendation on selecting the taper window parameters based on the obtained results.

6. COMPARATIVE ANALYSIS OF THE LFM PULSE COMPRESSION FILTERS WITH THE HAMMING AND BLACKMAN WINDOWS

As mentioned above, the window function given by Eq. (23) describes a wide class of taper windows applied for sidelobe suppression in the optimal LFM pulse compression filter. For further analysis, let us choose the Hamming and Blackman windows from all this variety which are most frequently used in radars. According to [5], the above window functions are as follows

a) Hamming window

$$w_H(t) = 0.53836 - 0.46164\cos(2\pi t/\tau_p), \quad (28)$$

b) Blackman window

$$w_B(t) = 0.7938 - 0.924\cos(2\pi t/\tau_p) + 0.143\cos(4\pi t/\tau_p). \quad (29)$$

The maximum sidelobe levels reported in [5] for windows in Eqs. (28) and (29) are equal to -42.6751 dB and -68.2361 dB, respectively. The amounts of loss in the signal-to-noise ratio, Γ_H and Γ_B, calculated for $w_H(t)$ and $w_B(t)$ after Eq. (27) are about -1.34 dB and -2.29 dB whose estimates agree well with the data of [5].

Figure 4 presents normalized signals $|S_{TwH}(t)|$ (upper panels) and $|S_{TwB}(t)|$ (lower panels) calculated for (a) $B = 32$ and (b) $B = 320$. The pulse length τ_p is equal to 3.2 μs in both cases.

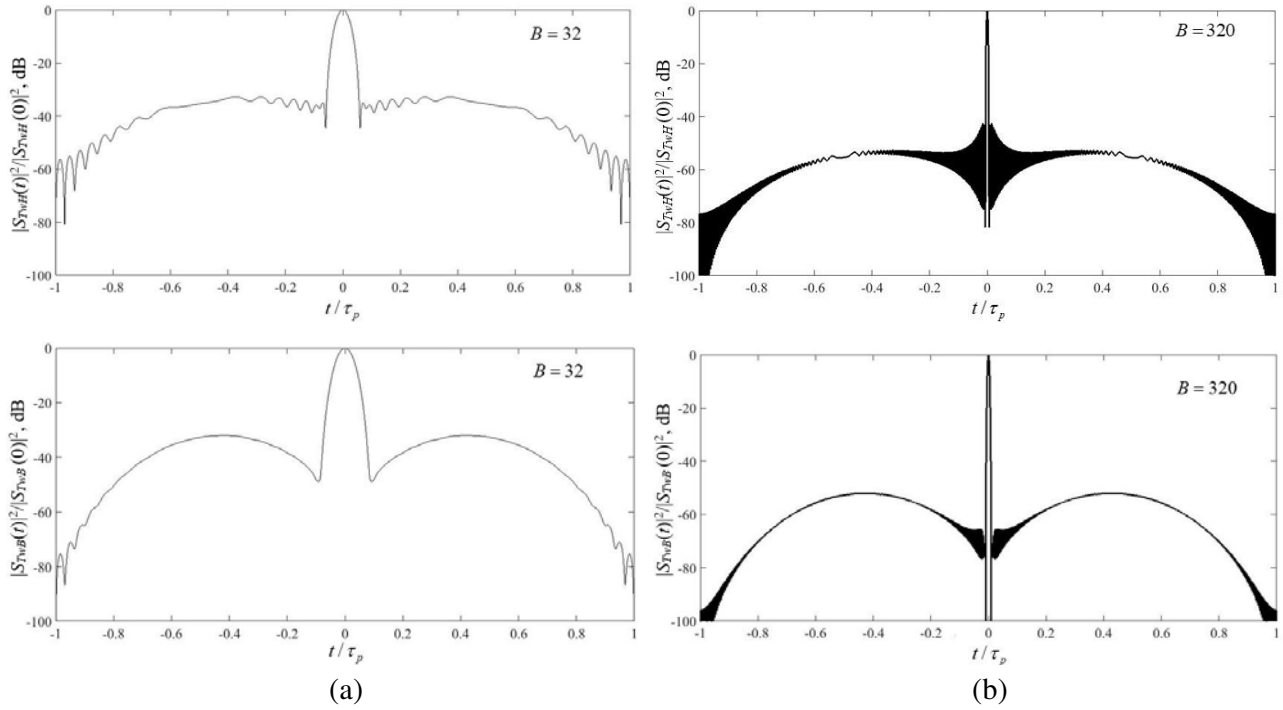

Figure 4. Signals $|S_{TwH}(t)|$ (upper panels) and $|S_{TwB}(t)|$ (lower panels) calculated for (a) $B = 32$ and (b) $B = 320$. The pulse length τ_p is equal to 3.2 µs in both cases.

As can be seen, the Blackman window more efficiently suppresses sidelobes in the vicinity of the main maximum as compared with the Hamming window. The charge for this is broadening of the main lobe. Thus, its relative width (normalized to that of $|S_{T0}(t)|$) estimated at -3, -20, and -40 dB levels for $B = 32$ makes, respectively, nearly 1.48, 1.65, and 1.82 for the Hamming window and 1.82, 2.01, and 2.49 for the Blackman window. With $B = 320$ the width at the -3 dB level remains practically the same, while at the -20 and -40 dB levels they are somewhat greater, approximately 1.69 and 1.95, respectively, for the Hamming window, and 2.15 and 2.76 for the Blackman window. The dependence $|S_{TwH}(t)|$ is more uniform, while $|S_{TwB}(t)|$ shows an essential increase near the points $t/\tau_p = \pm 0.5$. On the whole, the maximum sidelobe level for both windows considerably exceeds the values reported in [5]. Thus, with $B = 32$ it is about -32.69 dB for the Hamming window and -32.0 dB for the Blackman window instead of declared -42.6751 dB and -68.2361 dB, respectively. For $B = 320$, the efficiency of the Hamming window practically approaches the declared one (the maximum sidelobe level is about -42.49 dB), whereas that of the Blackman window remains essentially lower than that reported in [5] (the maximum sidelobe level is nearly -51.95 dB). It is noteworthy that with $B = 32$ the Hamming window proves to be more efficient, while for $B = 320$ the Blackman window is more efficient. Fig. 5 presents dependences of the maximum sidelobe level on the duration-bandwidth product B with $\tau_p = 4$ µs calculated for the Hamming (solid line) and Blackman (dashed line) windows. It is seen that the efficiencies of these windows become nearly equal with $B \approx 80$. With a further increase of B, the maximum sidelobe levels continue to decrease approaching the values reported in the literature [1, 5].

The behavior shown by the dependences in Fig. 5 allows supposing that by a purposeful selection of the parameters of the taper functions described by Eq. (23), it would be possible to somewhat improve the efficiency of standard taper windows applied for sidelobe suppression in the LFM pulse compression filter output. Most likely, in the case of small duration-bandwidth products B it would be necessary to solve the optimization problem individually for each specific value of B. As an example, Fig. 6 presents results of the compression of an LFM pulse with $B = 21$ calculated for the Hamming window (solid line) and a 3-term window with the coefficients $a_0 = 0.51$, $a_1 = 0.49$, and $a_2 = 0.001$ selected empirically. As can be seen, the main lobe width is practically equal to that observed for the Hamming window, while

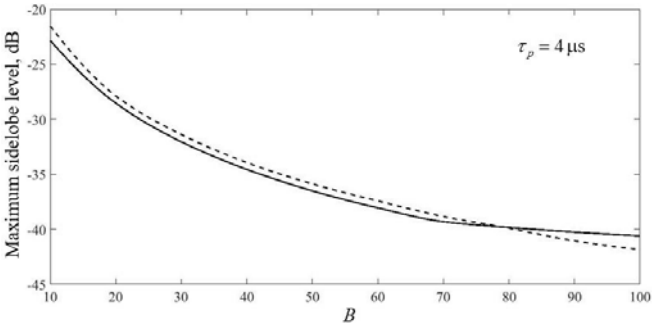

Figure 5. Maximum sidelobe levels calculated in dependence on the signal duration-bandwidth product B with $\tau_p = 4\,\mu s$ for the Hamming (solid line) and Blackman (dashed line) windows.

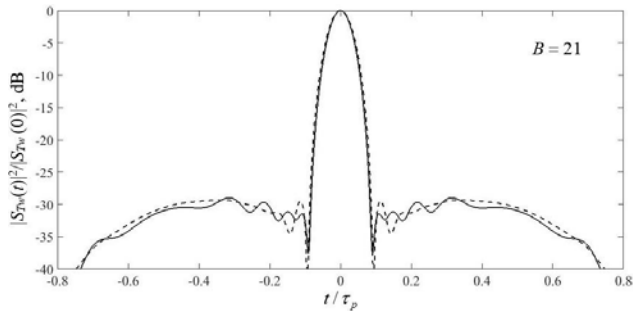

Figure 6. Results of compression of an LFM pulse with $\tau_p = 4\,\mu s$ and $B = 21$ using the Hamming window (solid line) and window $w(t) = 0.51 - 0.49\cos(2\pi t/\tau_p) + 0.001\cos(4\pi t/\tau_p)$ (dashed line).

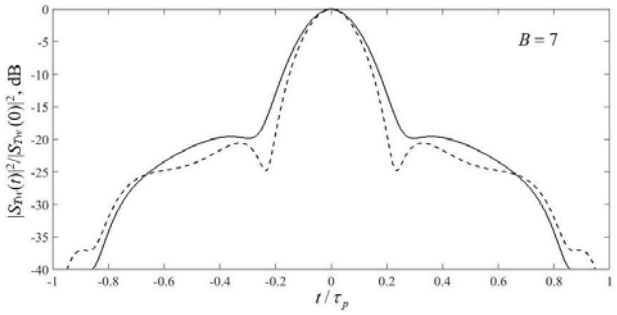

Figure 7. Results of compression of an LFM pulse with $\tau_p = 4\,\mu s$ and $B = 7$ using the Hamming window (solid line) and window (30) (dashed line).

the sidelobe level is lower by approximately 0.34 dB. Of course, the obtained efficiency gain is not so significant, but it is quite possible that a better result could be obtained using optimization techniques (see, for example, [10]). The suggested window keeps its advantage over the Hamming window within the range of B from 15 to 30.

A quite interesting result was obtained for the window

$$w(t) = 0.5375 - 0.33125\cos(2\pi t/\tau_p) - 0.09125\cos(4\pi t/\tau_p) \tag{30}$$

and duration-bandwidth product $B = 7$ (see Fig. 7). First, the gain in the sidelobe suppression efficiency was more than 1 dB (the maximum sidelobe level is -20.6 dB against -19.57 dB observed for the Hamming window). Second, the main lobe has proven to be narrower than that for the Hamming window. Thus, the width ratios at the -3 dB- and -18 dB-levels are about 0.88 and 0.79, respectively. It should be noted that an increase or a decrease of B results in that the window given by Eq. (30) becomes less efficient than the Hamming window. This fact confirms the assumption that the problem of taper window parameter optimization in the case of small duration-bandwidth products should be solved individually for each specific B.

7. CONCLUSIONS

The output of the optimal filter of the LFM pulse compression has been analyzed in order to look into the causes of inadequacy of the degree of sidelobe suppression using standard taper functions to the literature data. Expressions are presented for the positions of minima and maxima of the optimal filter response, as well as for the main lobe width. It is shown that the minima and maxima of the output signal are arranged symmetrically with respect to the time moments corresponding to the signal

propagation delay to the target and back plus/minus one half pulse length. Formulas are given for the maximum number of minima and maxima of the response of the optimum filter of LFM pulse compression and separation between adjacent and "like" (with the same numbers) minima and maxima in dependence on the signal duration-bandwidth product. It is shown that the separation between adjacent minima/maxima increases with their numbers. This effect is supposed to be responsible for the inadequacy of the efficiency of sidelobe suppression in the compressed LFM pulses to the literature-reported data. To validate this assumption, the output of the LFM pulse compression filter with the taper window in the form of an arbitrary real function has been calculated. It is shown that in order that the output signal be symmetric with respect to the pulse propagation time delay to a target and back the taper window function should be symmetric about the pulse center. The amount of loss in the signal-to-noise ratio due to the application of taper windows is estimated. The taper window function in the form of cosine harmonics of the Fourier series, which describes a rather great number of the standard windows, is analyzed in detail. An analytical expression has been derived for the output signal of the chirp-pulse compression filter on the basis of such windows, and a formula is presented for estimating the amount of loss in the signal-to-noise ratio. A comparative analysis of the Hamming and Blackman windows has been done in dependence on the pulse duration-bandwidth product B. It is shown that the application of Hamming window is more efficient up to $B \approx 80$ despite that the maximum sidelobe level reported in the literature for this window is considerably higher than for the Blackman window. For greater values of B, the Blackman window shows a higher efficiency. As B increases, the efficiency of both windows steadily increases asymptotically approaching the figure declared in the literature. Coefficients of taper window functions containing 2 cosine harmonics of the Fourier series have been empirically selected which made it possible to reduce the sidelobe level by approximately 0.34 dB for $B = 21$ and by more than 1 dB for $B = 7$ as compared with the Hamming window. The obtained results allow concluding that the optimization problem for the taper window parameters in the case of small signal duration-bandwidth products should be solved individually for each specific value of B. Most likely it would be impossible to obtain the extremely low sidelobe level; however, a certain improvement of the characteristics of the chirp-pulse compression filter seems quite possible. Future research might be focused on the use of optimization techniques for optimal selection of the taper window parameters in the case of comparatively small values of the pulse duration-bandwidth product.

REFERENCES

1. Cook, C. E. and M. Bernfeld, *Radar Signals: An Introduction to Theory and Application*, Academic Press, New York, 1967.
2. Barton, D. K., *Radar System Analysis and Modeling*, Artech House Publishers, Boston, 2004.
3. Ducoff, M. R. and B. W. Tietjen, "Pulse compression radar," *Radar Handbook*, M. I. Skolnik, ed., 8.1–8.44, McGraw-Hill Companies, New York, 2008.
4. Levanon, N. and E. Mozeson, *Radar Signals*, John Wiley & Sons, Inc., Hoboken, New Jersey, 2004.
5. Doerry, A. W., *Catalog of Window Taper Functions for Sidelobe Control*, Technical Report SAND2017-4042, Sandia National Labs., Albuquerque, New Mexico and Livermore, California, USA, 2017, DOI: 10.2172/1365510.
6. Tiwari, D. and S. S. Bhadauria, "Reduction in sidelobe and SNR improves by using digital pulse compression technique," *Int. J. Adv. Res. Sci. Eng.*, Vol. 6, No. 7, 1056–1063, 2017.
7. Kowatsch, M. and H. R. Stocker, "Effect of Fresnel ripples on sidelobe suppression in low time-bandwidth product linear FM pulse compression," *IEE Proc. F — Radar and Signal Processing*, Vol. 129, No. 1, 41–44, 1982, DOI: 10.1049/ip-f-1.1982.0007.
8. Rodionov, V. V., V. M. Rukavishnikov, Y. V. Filonov, E. A. Nikitin, M. A. Shilman, and V. N. Chesnov, "Method of radar signal processing," Russian Federation Patent No. 2212683, 2001.
9. Maurice, R. D. A., *Convolution and Fourier Transforms for Communications Engineers*, Pentech Press Ltd., London, 1976.
10. Reklaitis, G. V., A. Ravindranand, and K. M. Ragsdell, *Engineering Optimization. Methods and Applications*, John Wiley & Sons, Inc., New Jersey, 1983.